

Influence of Fuel Stratification on Turbulent Flame Propagation

Malik Hassanal^{*}, Venkat Raman,[†] Heeseok Koo,[‡]

The University of Michigan, Ann Arbor MI, USA

Meredith B. Colkett [§]

United Technologies Research Center, Hartford CT, USA

Flame propagation through variable equivalence ratio fuel/air mixtures is of importance in both stationary and aircraft gas turbine combustors. In this work, direct numerical simulation (DNS) is used to study the structure of a turbulence variable equivalence ratio flame, with the goal of understanding flame statistics under such conditions. The DNS uses homogeneous isotropic flow with mean streamwise velocity to emulate a flat flame propagation through unburnt fuel/air mixtures. It is found that when the stratification is present only at the large scales, flame evolution occurs through a series of fully premixed flames with varying equivalence ratios. On the other hand, when stratification occurs at the small scales, flame propagation is more complex with a very distorted flame front where low equivalence ratio structures lead to low temperature streaks that create secondary flame structures behind the main flow front.

I. Introduction

Fuel stratification is a physical phenomenon that has very high significance in both stationary and aircraft gas turbines, albeit for different reasons. In combustors for power generation, the fuel is premixed with compressed air and injected into the main combustion zone. Ideally, this high temperature flame is confined to a prescribed portion of the combustor. However, due to operational variations, there is a likelihood that the flame will propagate upstream of the combustion zone into the premixed section, which is not designed to hold high temperature gases and will thus lead to device failure. In combustors that use high hydrogen content fuels, this flashback occurs through flame propagation in the boundary layers. One strategy for arresting this flame flashback is through fuel stratification in the premixing zone, where lower fuel mass fraction is injected near the boundary layers which augments near-wall flame quenching.

Unlike stationary power turbines, aircraft engines predominantly use direct injection of liquid fuel into the combustion zone (although there is a trend towards more premixed designs). Due to the lag between fuel evaporation and combustion, finite mixing effects lead to a partially premixed or premixed flow configuration. Of direct interest here is the operation of such engines in sub-optimal conditions which generally occur at low power usage. Here, the spray cone used for injection issues into the combustor with a reduced pressure difference, which increases emissions. One theory for the source of these emissions is the ability of low equivalence ratio fuel/air pockets to go through the reaction zone without combusting or partially reacting, leading to the emission of species (unburnt hydrocarbons) that are otherwise not found in a fully burnt mixture. Here again, this process could be modeled as flame propagation through regions of variable equivalence ratio unburnt mixtures, which is essentially similar to the stratified flame process in a stationary gas turbine.

Based on this discussion, the objective here is to understand the structure of a turbulent premixed flame propagating through variable equivalence ratio mixtures. For this purpose, a homogeneous isotropic

^{*}Graduate Student, AIAA Member

[†]Associate Professor, AIAA Member

[‡]Post-doctoral fellow, AIAA Member

[§]Senior Research Fellow, AIAA Member

turbulence with uniform mean flow is considered. Direct numerical simulation of this configuration using detailed chemical kinetics is carried out for hydrogen/air combustion. Equivalence ratio fluctuations are introduced in two different ways to study the impact of the length scales of fluctuations on the flame front evolution.

The rest of the paper is organized as follows. Sec. II provides the simulation configuration and computational details including inflow turbulence and equivalence ratio fluctuation generations. Results are presented in Sec. III, followed by an Appendix that describes how the flame position is controlled in the domain.

II. Simulation configuration

The effect of fuel stratification on flame propagation is studied using DNS with detailed chemical mechanism. The DNS cases studied use a computational domain that is periodic in the y and z directions, and has an inflow and outflow in the x direction (streamwise direction). The computational domain spans $0.5h \times h \times h$ in the streamwise, streamnormal and spanwise directions, where $h = 4\text{cm}$. The flame front location is controlled using a closed-loop feedback algorithm that adjusts the inflow velocity such that the flame is contained within a short region in the streamwise direction. Hence, the streamwise length is shorter compared to the other two directions. The computational grid $256 \times 512 \times 512$ in the three directions, respectively. At stoichiometric conditions, the flame thickness is four times the grid spacing, and the Kolmogorov length scale, assuming isotropic flow, is roughly twice the size of the grid spacing. Figure 1 shows the dimensions of the computational domain.

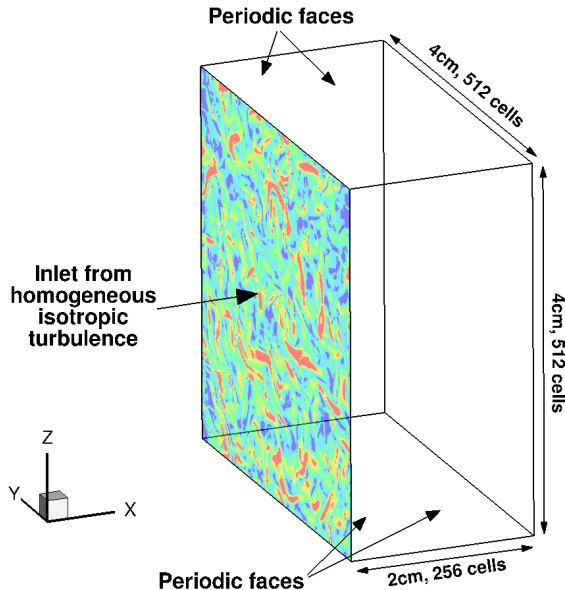


Figure 1. Sketch of the computational domain, with instantaneous vorticity plotted on the inlet plane. Inlet condition is from a homogeneous isotropic turbulence DNS.

The DNS computations were carried out using the low-Mach number solver NGA.¹ The governing equations are cast in a low-Mach number formulation, whereby the acoustic wave propagation is removed from the system of equations. For the cases studied here, the use of the low-Mach number solver is justified because the flow velocity is small compared to the acoustic wave propagation speed and the configuration is not confined by walls. A detailed chemistry model using 19 steps and 9 reactive species is used for hydrogen combustion.² The flow solver is second-order accurate in both space and time.³ Convection term for equivalence ratio transport equation is solved by QUICK scheme.

The inflow boundary conditions require more description. Macroscopically, a mean flow velocity that is roughly $2.3S_l$, where S_l is the laminar flame speed at stoichiometric conditions, is imposed. To generate time and space correlated structures at the inflow, a separate homogeneous isotropic turbulence (HIT) is used. The HIT is performed at $Re_\lambda = 40$ on a uniform 128^3 mesh. It was taken care to ensure that the grid was sufficiently resolved to support the range of length scales for this Reynolds number. Since the

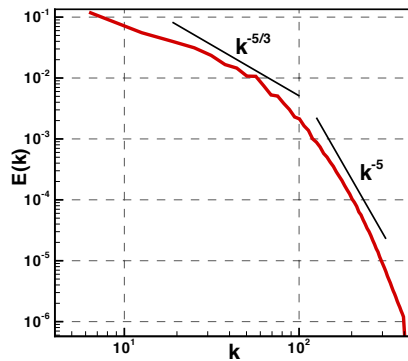


Figure 2. Spectrum of HIT DNS for inflow velocity boundary condition generation.

numerical algorithm is energy conserving, lack of resolution should technically lead to energy pile-up at the small scales, which was not observed here. The size of the box is h , which is identical to the y - z plane size in the main flame simulation. The Kolmogorov lengthscale is roughly half of the grid size, indicating that the grid resolution is four times coarser than the reacting DNS. A linear forcing is imposed^{4,5} until the turbulence is in a statistically stationary state. The kinetic energy spectrum corresponding to this HIT is given in Fig. 2. It is seen that in spite of the coarse mesh size, a small region of inertial range scaling is found, followed by the steeper decay of energy associated with the dissipation scales. The inflow turbulent field is stored in a file and read by the main DNS such that turbulent lengthscales are kept the same. It includes an assumption that the bulk streamwise velocity does not alter the turbulent information. With this approach, a DNS with a controlled flame location is equivalence to a stationary turbulence through which a flame front evolves⁶ in space. For all the computations, the flame front is initialized as a thin sheet, with a regularized jump condition applied over five grid points in the streamwise direction. This is close to the real flame thickness under stoichiometric conditions. Initially, density and velocity conditions across the flame front are carefully selected to ensure mass and momentum conservations.

Two different cases with stratification was studied, named large scale stratification (LSS) and small scale stratification (SSS). For both these cases, the inflow turbulent field fed to the main flame simulation is identical, but the difference lies in the introduction of the scalar field. The objective of these studies is to introduce equivalence ratio fluctuations such that the flame front experiences time-evolving fuel-to-air ratios. In the case of the LSS, the fuel-air ratio is introduced as a uniform value in the inlet plane but changes in time from an initial value of 2 to 0 over 1ms, which is roughly equivalent to 3/4 of a flow-through time. In the SSS case, a spectrum of length scales is used to generate a three-dimensional scalar field of mixture

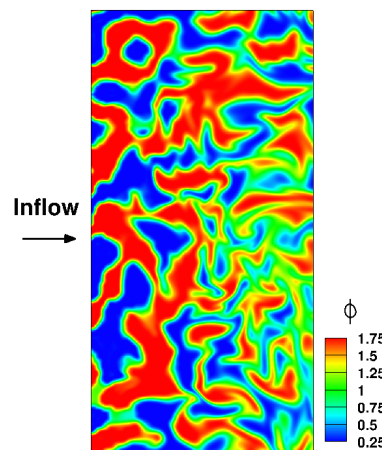


Figure 3. A decaying passive scalar field transported using a turbulent flow field in the streamwise direction.

fraction, which is then fed to the inlet plane of the flame simulation. The scalar field is generated with in a similar manner to Eswaran and Pope.⁷ The model spectrum is in Gaussian centered by a length scale that contains the dominant energy, which is specified as $h/12$ in this study. This scalar field is directly carried into the domain with the developed velocity fields. The scalar is rescaled such that the maximum and minimum equivalence ratios are 0.25 and 1.75, respectively. Without reaction, the scalar evolves in the domain as depicted in Fig. 3.

III. Results and discussion

A. Large scale stratification (LSS)

The LSS case involves large scale variation of the equivalence ratio. Due to the nature of the flow, these variations do not cascade down to the small scales in the distance between the inlet and the flame, and retain much of their large scale features. Figure 4 shows the evolution of the flame front with time. The domain is initialized with an equivalence ratio of 2, which is progressively replaced by lower values as the inflow conditions change with time. As the equivalence ratio seen by the flame initially moves towards stoichiometric condition, the flame is seen to become thinner, with increased source terms and peak temperatures. Note that resolution of the DNS is chosen such that the thinnest flame zone is adequately captured by the grid.

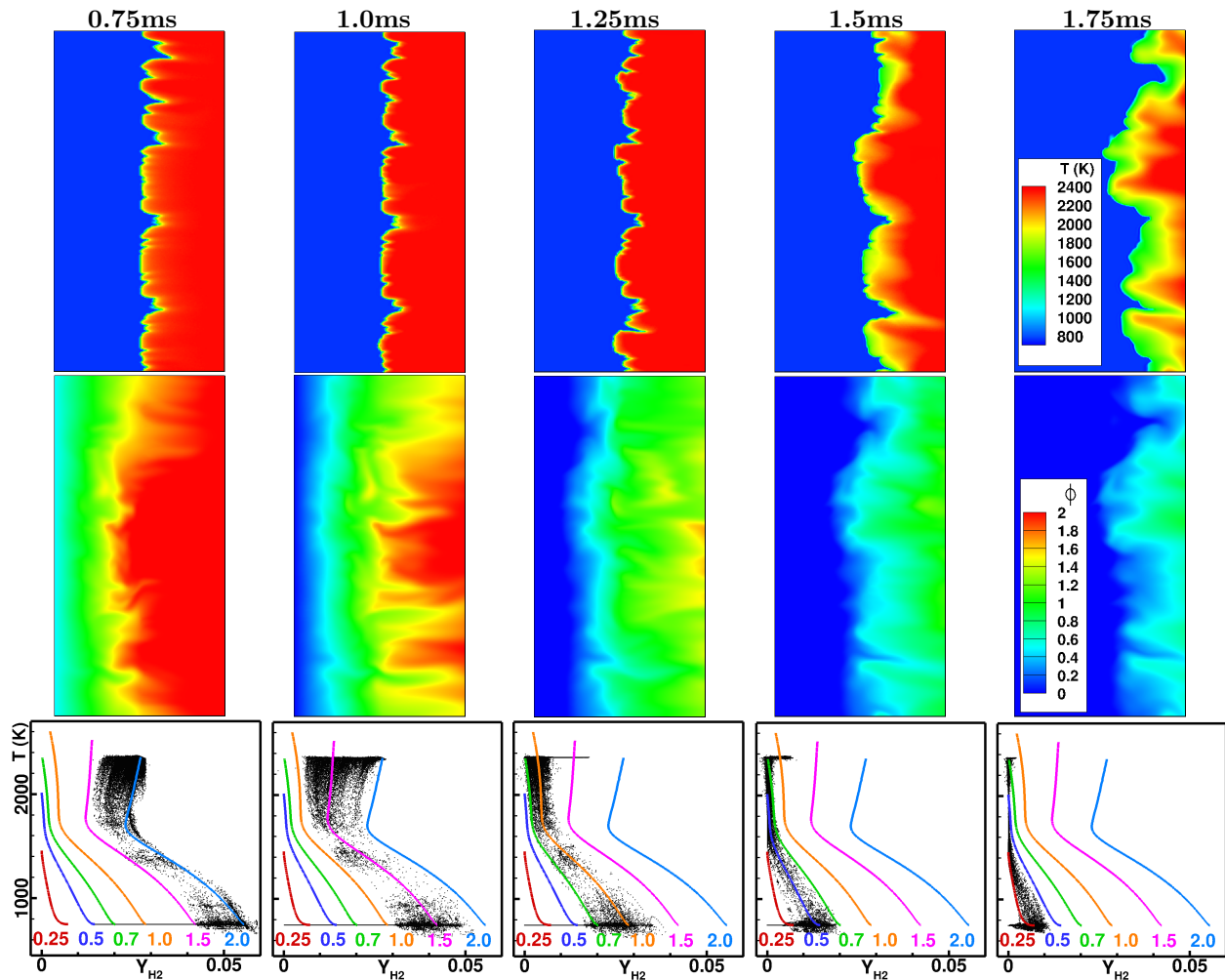


Figure 4. (Top) Temperature and (middle) ϕ and (bottom) composition space plots at different times from the initial condition. Several flamelet solutions for different ϕ 's between 0.25 and 2 are plotted on top of the composition space plots. Inflow ϕ varies between 0ms and 1ms, from 2 to 0.

As the equivalence ratio further drops, the flame front becomes broader with lower temperatures across the front. The post-flame temperature is also lower indicating increased dilution of heat release. Beyond the lower flammability limit, the flame extinguishes as expected.

Figure 5 shows the evolution of the flame isosurface corresponding to a temperature of 1000K. In the initial phase of the simulation, the strong combustion leads to heat-release generated small-scale structure that causes extensive flame wrinkling. It is also seen that the post-flame velocities can reach velocities up to three times the inflow velocity, corresponding to gas expansion from heat release. This strong streamwise gradient in velocity generates the vortex structures that cause flame wrinkling. As the equivalence ratio decreases, heat release is also reduced, which affects the post-flame velocities. As seen in Fig. 5, at later time, the post-flame velocities do not increase substantially beyond the inflow velocities. Consequently, flame wrinkling is also reduced leading to lower equivalent turbulent burning velocity. It is important to note that this reduction in surface area further decelerates the flame, pushing the system towards extinction.

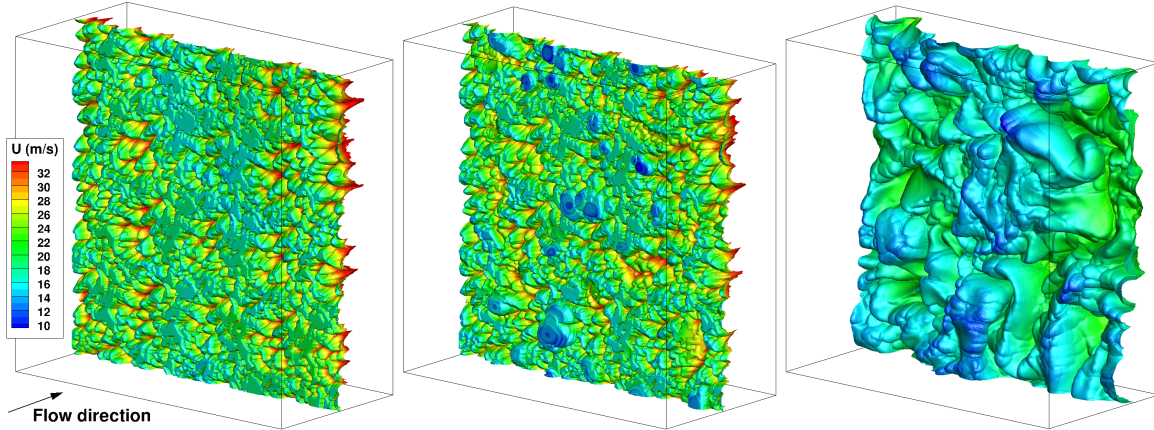


Figure 5. Isosurface of temperature (1000K) colored by the local streamwise velocity, corresponding to the first, third, and fifth timeframe in Fig. 4.

Figure 4 also shows the comparison in composition space between the DNS and premixed flamelet calculations. The flamelet solutions were obtained at different equivalence ratios for a one-dimensional system with identical chemistry mechanism. Interestingly, the scatter plot in composition space follows closely the flamelet solution. At different times, the flame front experiences different equivalence ratios, which is reflected in the composition space plot where the scatter aligns with different premixed flamelet solutions. This confirms the notion that large scale equivalence ratio variations could be seen as merely a collection of propagating premixed flames at different equivalence ratios. In this sense, the structure of the flame is not affected by stratification.

B. Small scale stratification (SSS)

The SSS case presents a different scenario, where the integral length scale of the scalar structures are roughly 10 times the grid spacing. Here, the equivalence ratio fluctuations occur at scales comparable to the flame thickness, which implies that strong variations could occur where the chain branching reactions take place. Note that this flame is statistically stationary as opposed to the LSS case that is time evolving due to the changes in the inflow conditions. Figure 6 shows the temperature, equivalence ratio, and streamwise velocity fields in a two-dimensional plane at the center of the spanwise direction. It is seen that the flow retains the small scale variations in equivalence ratio as it encounters the flame. The flame front is more complex than that for the LSS case, with regions of very low temperature corresponding to the presence of low equivalence ratio fuel/air mixture. Since the length scale of these structures are comparable to the flame thickness, low temperature streaks are found to penetrate deeper in the streamwise direction.

Figure 7 shows the isocontours of temperature for the SSS case. Compared to the same plot for the LSS case (Fig. 5), the SSS case shows larger structures. This is mainly due to the low or high equivalence ratio regions that have reduced heat release compared to stoichiometric mixture. This reduces the gas expansion and the post-flame velocity and the velocity gradients across the flame, which reduces flame wrinkling. The

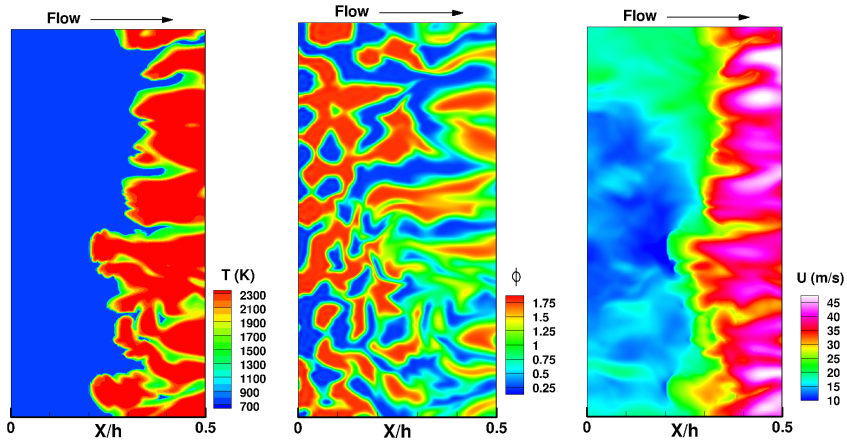


Figure 6. Instantaneous temperature, equivalence ratio, and streamwise velocity plotted at the center plane in the spanwise direction.

presence of the small scale structures distinctly changes flame evolution. If the equivalence ratio falls below the flammability limit, this will introduce flame holes that will propagate and mix with the burnt gases post flame. If this mixing happens with higher than stoichiometric but burnt regions, a secondary flame zone could be formed. Hence, such intense stratification is fundamentally different from the LSS case.

Figure 8 shows the composition space plot similar to that for the LSS. It is seen that the flame front now spans a number of different flamelets, with the flame front found at a number of different equivalence ratios. The composition plot itself does not describe the structure of the flame, which shows structures that are not typically observed in premixed flames (Fig. 7). A more detailed analysis of the Lagrangian trajectories of the fluid particles are being carried out now.

IV. Conclusions

Direct numerical simulation of flame front propagation in premixed flames was carried out, but with the added complexity of fuel stratification. For hydrogen/air flames, flame evolution in a periodic box with mean convective velocity was performed. A control algorithm to position the flame at a required streamwise location is used. It was verified that the algorithm correctly positions the flame for a one-dimensional laminar flame. The turbulent flame propagation was studied using two different inflow conditions for the

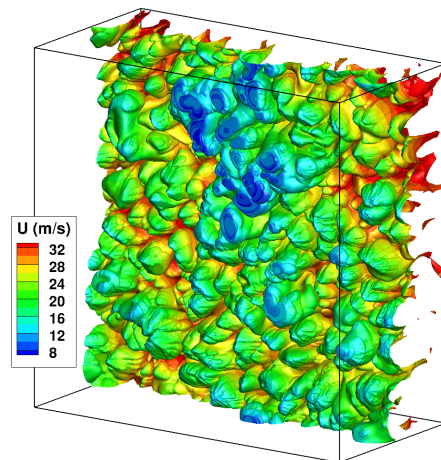


Figure 7. Isosurfaces of temperature (1000K) colored by the local streamwise velocity.

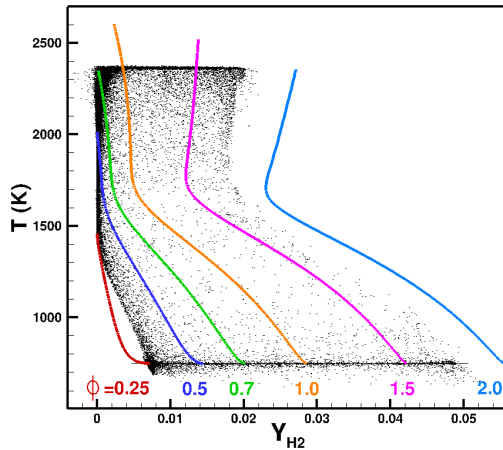


Figure 8. Conditional plot from SSS compared to flamelet solutions for different equivalence ratios.

scalars. When the stratification was essentially large scale dominated, the inflow was specified such that the equivalence ratio is uniform at the inlet plane but changed with time. In this case, the flame evolution was found to be similar to a succession of fully premixed flames with varying equivalence ratios. In the case when stratification occurs at the small scales, the flame front exhibits variations in peak temperature consistent with the local fuel/air ratio. In addition, flame wrinkling is considerably reduced compared to uniform but near-stoichiometric equivalence ratio conditions due to the reduction in post-flame velocities and the associated gradients in the streamwise direction. Overall, the physical structure of the flame is found to be different from the large scale stratification case.

Appendix: Control algorithm for flame placement

In order to ensure that the flame encounters the same turbulent flow statistics for the entire duration of the simulation, its position is controlled using a control algorithm. The control algorithm relies on introducing a correction velocity at the inflow to counter flame motion away from the control point. The procedure is based on the algorithm introduced by Bell et al.⁸ In this work, a controller with a static gain equal to 1 is used. The control block is shown in Fig. 9.

This control procedure can be derived by recognizing that the local elementary variation of the flame position can be written in terms of the local flow velocity and the local flame velocity as

$$\Delta h = (U_{in} - s_T)dt, \quad (1)$$

where h is the flame position, U_{in} is the local flow velocity encountered by the flame front and s_T is the local turbulent flame velocity. For use in the control algorithm, a response time τ is defined. This time should

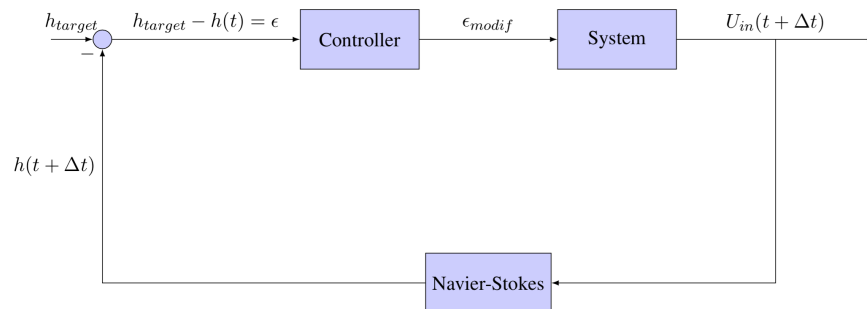


Figure 9. Block diagram describing the control loop.

be interpreted as the time between the moment where the convection velocity correction is applied and the moment where the flame position is effectively corrected. This response time τ is expressed in terms of the simulation timestep as

$$\tau = K\Delta t, \quad (2)$$

where Δt is the simulation timestep and K is a constant greater than 1. It was found that values of K close to 4 gave stable and accurate results. Based on this response time, the convective velocity to impose at the inlet is simply expressed by

$$U_{in}(t + \Delta t) = 2\frac{\epsilon}{K^2\Delta t} - 2\frac{\Delta h}{K\Delta t} + U_{in}(t), \quad (3)$$

where ϵ is the difference between the intended flame location (in x distance) and the current flame location. In the above equation, the first term of the right hand side is the contribution of the global error in the flame position. The second term is the contribution of the instantaneous variation of the flame position. It can be seen from Eq. 3 that those two contributions have opposite sign. Thus, as the flame gets closer from the target position, the correction is progressively damped which reduces the flame oscillations around the target position. Note also that since $K > 1$, the dominant term of the convective velocity correction is due to the instantaneous flame position variation. The convective velocity is then actively corrected at each timestep. It is therefore important to generate turbulent inflow independent of the mean convective velocity (described in Sec. II). The formula presented for the control algorithm does not explicitly require an estimation of the turbulent flame velocity. However, this quantity can be easily obtained by approximating Eq. 1 with

$$s_T = U_{in}(t) - \frac{\Delta h}{\Delta t}. \quad (4)$$

To validate the algorithm used here, a 1D flame configuration with detailed chemistry has been simulated. A premixed hydrogen/air mixture with equivalence ratio of 0.55 is used. The inlet temperature is set to 750 K and the configuration operates at 2 atm. For this configuration, the expected laminar flame speed is 6.67 m/s as obtained from a one-dimensional steady calculation using the FlameMaster code.⁹ The flame is initialized at $X = 15$ mm and the target flame position is $X = 7.5$ mm. By intentionally initializing the flame at a location other than the set point, it is possible to understand the efficiency of the algorithm in controlling the flame position. The flame is resolved using the same number of points as in the full-scale DNS described in Sec. II.

Figure 10 shows the specified convection velocity at the inlet based on the control algorithm and the variation in the estimated flame velocity. In the first few time-steps, the flame propagates towards the target position. During this time, the control velocity is set to zero since the flame is moving upstream towards the set point. When the flame is close to the set location, the control velocity starts to increase to prevent the flame from propagating further upstream. After that, the damping algorithm ensures that the flame does not move too far from the set point, and the control velocity finally reaches the asymptotic value close to the laminar flame speed.

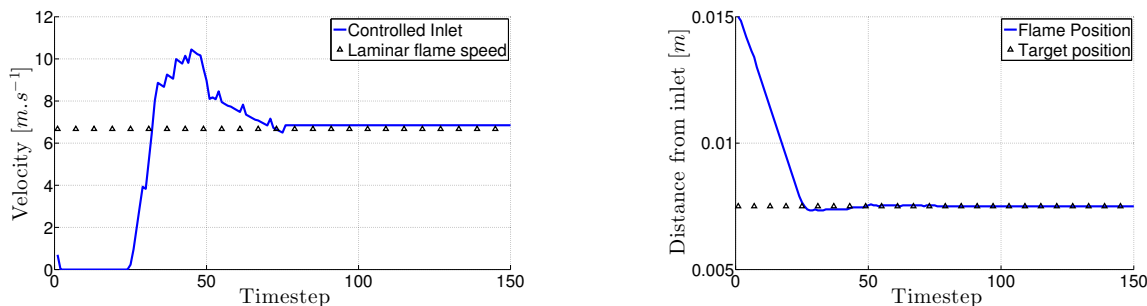


Figure 10. Variation of (left) inlet velocity and (right) flame position with time.

References

- ¹Desjardins, O., Blanquart, G., Balarac, G., and Pitsch, H., "High order conservative finite difference scheme for variable density low Mach number turbulent flows," *Journal of Computational Physics*, Vol. 227, No. 15, JUL 20 2008, pp. 7125–7159.
- ²Mueller, M., Kim, T., Yetter, R., and Dryer, F., "Flow reactor studies and kinetic modeling of the H-2/O-2 reaction," *International journal of chemical kinetics*, Vol. 31, 1999, pp. 113–125.
- ³Pierce, C. D., *Progress-variable approach for large-eddy simulation of turbulence combustion*, Ph.D. thesis, Stanford University, 2001.
- ⁴Lundgren, T. S., "Linearly forced isotropic turbulence," *Annual Research Briefs*, 2003, pp. 461–473.
- ⁵Rosales, C. and Meneveau, C., "Linear forcing in numerical simulations of isotropic turbulence: Physical space implementations and convergence properties," *Physics of Fluids*, Vol. 17, 2005.
- ⁶Hamlington, P. E., Poludnenko, A. Y., and Oran, E. S., "Interactions between turbulence and flames in premixed reacting flows," *Physics of Fluids*, Vol. 23, 2011, pp. 125111.
- ⁷Eswaran, V. and Pope, S. B., "Direct Numerical Simulations of the Turbulent Mixing of a Passive Scalar," *Physics of Fluids*, Vol. 31, 1988, pp. 506.
- ⁸Bell, J. B., Day, M. S., Grcar, J. F., and Lijewski, M. J., "Active control for statistically stationary turbulent premixed flame simulations," *Communications in Applied Mathematics and Computational Science*, Vol. 1, 2006, pp. 29–51.
- ⁹Pitsch, H., "A C++ Computer Program for 0-d and 1-D Laminar Flame Calculations," RWTH Aachen.